Journal of Power Sources 242 (2013) 581–588

Contents lists available at SciVerse ScienceDirect

Journal of Power Sources

journal homepage: www.elsevier.com/locate/jpowsour

Tailoring electrode hydrophobicity to improve anode performance in alkaline media

Matt S. Naughton, Geun Ho Gu, Akash A. Moradia, Paul J.A. Kenis*

Department of Chemical & Biomolecular Engineering, University of Illinois at Urbana-Champaign, 600 South Matthews Ave, Urbana, IL 61801, USA

HIGHLIGHTS

- Backing layers may be permeable to catalyst solvent.
- 20 wt% PTFE optimal for alkaline anode.
- High hydrophobicity limits anode performance.
- Hydrophobic anion-conducting binder inferior to Nafion.
- PtRu potentially very good anode catalyst.

ARTICLE INFO

Article history:
Received 15 February 2013
Received in revised form
9 May 2013
Accepted 13 May 2013
Available online 29 May 2013

Keywords:
Alkaline fuel cell
Gas diffusion electrodes
Electrode characterization
Reference electrode
Hydrophobicity
Water management

ABSTRACT

Limitations in anode performance have been a major obstacle to widespread alkaline fuel cell usage. In contrast to water management in acidic cathodes, water management in alkaline anodes has not received a lot of attention. Here, we use a methodology based on individual electrode plots to analyze and improve anode performance, especially by changing the hydrophobicity. Specifically, we determine the role of hydrophobicity as it affects performance for backing layers, catalyst layers, and catalyst binders. We use both individual electrode plots and recirculating experiments to determine the optimal PTFE loading was 20 wt% in alkaline media. We investigated PTFE and Fumion binders, determining that their use yields higher overpotentials than when using Nafion in alkaline media. Furthermore, we determined that Nafion alternatives for application in alkaline media would require significant hydrophilicity and anion-conductivity to result in good fuel cell performance.

1. Introduction

Alkaline fuel cells are showing substantial promise as power sources due to superior cathode kinetics and improved stability of non-noble metal catalysts in alkaline media [1–5]. While adverse effects of carbon dioxide reacting with hydroxide have historically been perceived to substantially limit alkaline fuel cell performance, more recent developments have demonstrated that the effect of carbonate formation can be mitigated by using soda lime scrubbing [6], a membrane without free cations [7], or a flowing electrolyte with a large electrolyte volume [8]. Performance limitations of alkaline fuel cells at higher current densities then stem more from anode limitations, as the anode is the electrode where water formation occurs [9].

Previously, the role of hydrophobicity on performance of the cathode in acidic fuel cells has been examined [10]. These cathodes are prone to flooding issues analogous to an alkaline anode. A study by Li et al. examined the effect of silicone oil on cathode performance [11]. Zhang et al. investigated the role of PTFE in the cathode backing layer [12]. Fairweather et al. determined that PTFE wet-proofing at less than 20 wt% did not cause a substantial loss in electrode porosity [13]. While these studies yielded information about the cathode in acidic media, their results did not discuss applicability to alkaline media.

We have previously developed a microfluidic hydrogen-oxygen (H_2/O_2) fuel cell with a flowing alkaline electrolyte stream [14]. This cell has the versatility of a three electrode cell within an operating fuel cell. More recently, we have developed a method to analyze individual electrodes by plotting their overpotential versus a

* Corresponding author. Tel.: +1 217 265 0523; fax: +1 217 333 5052.
E-mail address: kenis@illinois.edu (P.J.A. Kenis).

0378-7753/$ – see front matter © 2013 Elsevier B.V. All rights reserved.
http://dx.doi.org/10.1016/j.jpowsour.2013.05.054

reference electrode. We have used this method to determine the effects of electrolyte contamination and cathode catalysts on performance [8,9], but we have not focused on using this methodology to improve anodes.

In this work, we use the aforementioned microfluidic H_2/O_2 fuel cell to characterize the effect of hydrophobicity of the electrode on anode performance. Specifically, we tune the hydrophobicity both in the backing layer and in the catalyst layer of an electrode to obtain optimal performance. The effect of PTFE loading is investigated both for polarization curves of single electrodes as well as for 4.5 h whole-cell experiments using a recirculating electrolyte. Furthermore, we activated and tested alternate binders to determine their effects on electrode performance.

2. Experimental

2.1. Gas diffusion electrode preparation

Commercially available Pt/C (50% mass on Vulcan carbon, Alfa Aesar) was used as cathode and anode catalyst. For one trial, PtRu/C (50% Pt mass, 25% Ru mass on Vulcan carbon, Alfa Aesar) was used as the anode catalyst in place of Pt/C. Unless otherwise stated, a 30:1 ratio of catalyst to Nafion was used as the catalyst binder such that catalyst inks were prepared by mixing a total of 8.0 mg of Pt/C (or PtRu/C) and 6.13 μL of 5 wt% Nafion solution (DuPont) [2,15]. 200 μL of DI water and 200 μL of isopropyl alcohol (Fisher Scientific) were added as carrier solvents. The catalyst inks were sonicated (Sonics Vibra-Cell) for 10 min to obtain a uniform mixture, which was then hand-painted onto 4 cm^2 of the hydrophobized carbon side of a carbon paper gas diffusion layer (35 BC, SGL carbon group or Toray TGP-H-060) to create a gas diffusion electrode (GDE). The final catalyst loading was 1 mg cm^{-2} of Pt (50% mass Pt) for each electrode.

2.2. Fuel cell assembly and testing

To assemble the fuel cell, shown in Fig. 1, the cathode (Pt/C) and the anode (Pt/C) were placed on the opposite sides of a polymethylmethacrylate (PMMA) window (0.15 cm thick unless otherwise specified), such that the catalyst-coated GDE sides face the 3 cm long and 0.33 cm wide window machined in PMMA [15]. The microfluidic chamber volume was 0.15 ml (0.2 or 0.1 ml when using a 0.2 or 0.1 cm thickness separator, respectively). The window has one inlet and one outlet from the side for the electrolyte flow, aqueous solutions of potassium hydroxide (KOH, Sigma–Aldrich, 85%, balance of H_2O). Two 1 mm thick copper-infused graphite windows were used as current collectors. Polycarbonate gas flow chambers (5 cm (L) × 1 cm (W) × 0.5 cm (H)) were used to introduce both hydrogen and oxygen gases (laboratory grade, S.J. Smith), at 10 SSCM each. The multilayer assemblies were held together with binder clips. Fuel cell testing was conducted using a potentiostat (Autolab PGSTA-30, EcoChemie) at room temperature. For all studies, electrolyte flow rate was maintained at 0.6 ml min^{-1} either using a syringe pump (2000 PHD, Harvard Apparatus) or a recirculating piston pump (MCP-CPF with MFI 009 Pump Head, Harvard Apparatus). Fuel cell polarization curves were obtained by measuring steady-state currents at different cell potentials using Nova software (EcoChemie). The exposed geometric surface area of the electrode (1 cm^2) was used to calculate the current and power densities. A reference electrode (Ag/AgCl in saturated NaCl, BASi) was placed at the outlet of the electrolyte stream to allow for the independent analysis of polarization losses on the cathode and the anode [14]. The reference electrode was fitted with a polyethylene frit (Princeton Applied Research) in place of the original Vycor® frit to prevent corrosion and contamination in alkaline media [9]. After each experiment, the fuel cell was disassembled and the electrodes were rinsed with deionized water, then dried for at least 30 min under a laboratory fume hood.

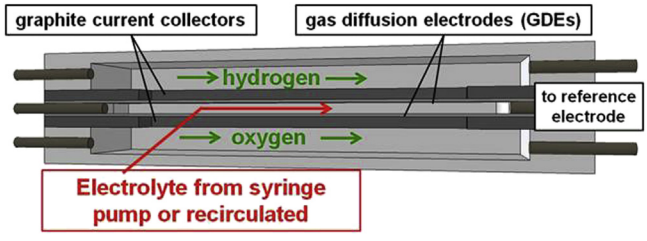

Fig. 1. Diagram of a microfluidic fuel cell with a flowing alkaline electrolyte.

3. Results and discussion

3.1. Effect of electrode backing layers

The backing layer can play a major role in determining gas diffusion electrode properties. Beyond the basic properties of porosity and thickness, the deposition of the catalyst layer can vary greatly based on the structure of the backing layer. Surprisingly, this variance can occur for backing layers with the same specifications. Originally, the electrodes synthesized with the Sigracet 35 BC backing layers performed well, with overpotentials below 0.1 V for current densities below 50 mA cm^{-2} as shown in Fig. S1. However, electrodes created out of subsequent orders of Sigracet 35 BC yielded very high overpotentials and maximum current density below 150 mA cm^{-2} (Fig. S1). This poor performance is consistent with mass transport limitations at the anode, due to the steep upward trend deviating from linearity.

Many (>10) electrodes were painted to investigate whether this low performance was caused by poor painting technique. Although steps such as painting over 5 h, heating the electrodes to facilitate solvent evaporation, blowing nitrogen over the surface, and using smaller brushes were tried, none of these steps solved the problem or improved the electrode performance. Ultimately, the high performance from the previous batch was restored by switching to a different backing layer, Toray TGP-H-060 (Fig. S1). This backing layer contains 10 wt% PTFE, versus 5 wt% for Sigracet, and lacks the microporous layer found in the Sigracet. Fig. S1 shows the similar overpotentials for Toray and the original Sigracet electrodes. Although IR-corrections are possible based on our previous work [9], the overpotentials are shown as measured because the emphasis is on the difference between the newer Sigracet backing layer performance and the Toray performance. Subsequent anode overpotentials are not IR-corrected due to the identical electrolyte thickness and composition used in each set of experiments, indicating that the IR losses are identical.

The cause of this improved Toray performance was investigated through hydrophobicity testing. By placing a droplet of deionized water on the backing layer, the contact angle between the water and the backing layer was obtained. Fig. 2 shows that both the Sigracet and Toray backing layers are hydrophobic, with contact angles above 90 °C. The difference between the layers stems from their behavior in the presence of the 50:50 IPA:H_2O catalyst ink mixture. The Sigracet backing layer rapidly absorbs the catalyst ink mixture, which leads to flooding during cell operation and thus the mass transport limitations observed in Fig. S1. The Toray backing layer does not absorb the catalyst ink to the same degree, so the backing still allows gas transport during cell operation. This difference in behavior is the cause of the superior Toray performance.

Backing layer / solvent	Sigracet 35 BC	Toray
Water	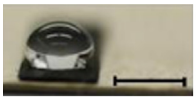 5 wt% PTFE	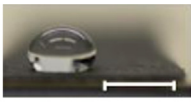 10 wt% PTFE
50:50 IPA:water	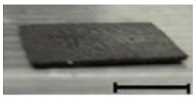 5 wt% PTFE	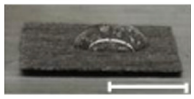 10 wt% PTFE
50:50 IPA:water	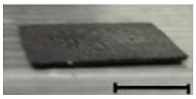 5 wt% PTFE	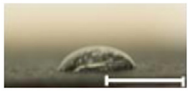 5 wt% PTFE

Fig. 2. Comparative hydrophobicity of Sigracet and Toray backing layers in the presence of water and a 50:50 water-IPA mixture. Scale bars are approximately 0.5 cm.

Further investigation was used to determine whether the higher wt% PTFE in the Toray or the lack of a microporous layer was responsible for the improved Toray performance. Toray carbon paper with 5 wt% PTFE was used to create electrodes with the same Pt and PTFE loading as the Sigracet electrodes. When these electrodes were subjected to the hydrophobicity test with the catalyst solvent, the 5 wt% PTFE Toray backing layer showed solvent resistance similar to the 10 wt% PTFE (Fig. 2). This behavior demonstrates that the poor solvent tolerance of the Sigracet 35 BC is due to the structure of the layer, as opposed to the PTFE content. Even with the Toray backing layer, the electrode performance is very sensitive to painting time; further information is given in Section S1.

When translating these results to membranes, these results would be expected to apply to catalyst-painted backings but not catalyst-coated membranes. When depositing the catalyst on electrodes, the same hydrophobicity-related flooding issues for Sigracet 35 BC would apply whether the electrode is exposed to a liquid electrolyte or a solid membrane. Thus, the catalyst buildup inside the backing layer would cause flooding and limit current density for membrane systems as well. However, the analogous problem of electrolyte weeping, where the electrolyte diffuses out of the backing layer, would not pose a problem for membrane-based systems. For catalyst-coated membranes, the flooding issues would not appear to the same degree, since the catalyst ink solvent does not contact the backing layer for a catalyst-coated membrane.

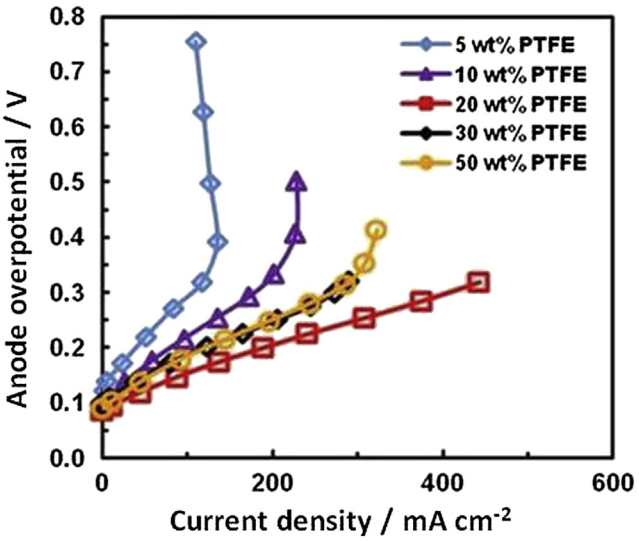

Fig. 3. Anode overpotential as a function of current density for varying PTFE wt%. Electrolyte: 3 M KOH. Electrolyte flow rate: 0.45 ml min^{-1}. Electrolyte thickness: 1.5 mm H_2/O_2 feeds: 50 SCCM. At room temperature.

3.2. Effect of varying PTFE wt% on backing layer overpotential

After the previous study, the effect of backing layer PTFE content was investigated. Using more PTFE increases the hydrophobicity of the backing layer at the expense of weakening catalyst adhesion and increasing electrical resistance [12]. Electrodes were synthesized using Toray TGP-H-060 backing layers and tested in the microfluidic fuel cell. Fig. 3 shows that the highest overpotential comes from the 5 wt% PTFE backing layer, with the optimal performance (lowest overpotential) found at 20 wt% PTFE. Above this

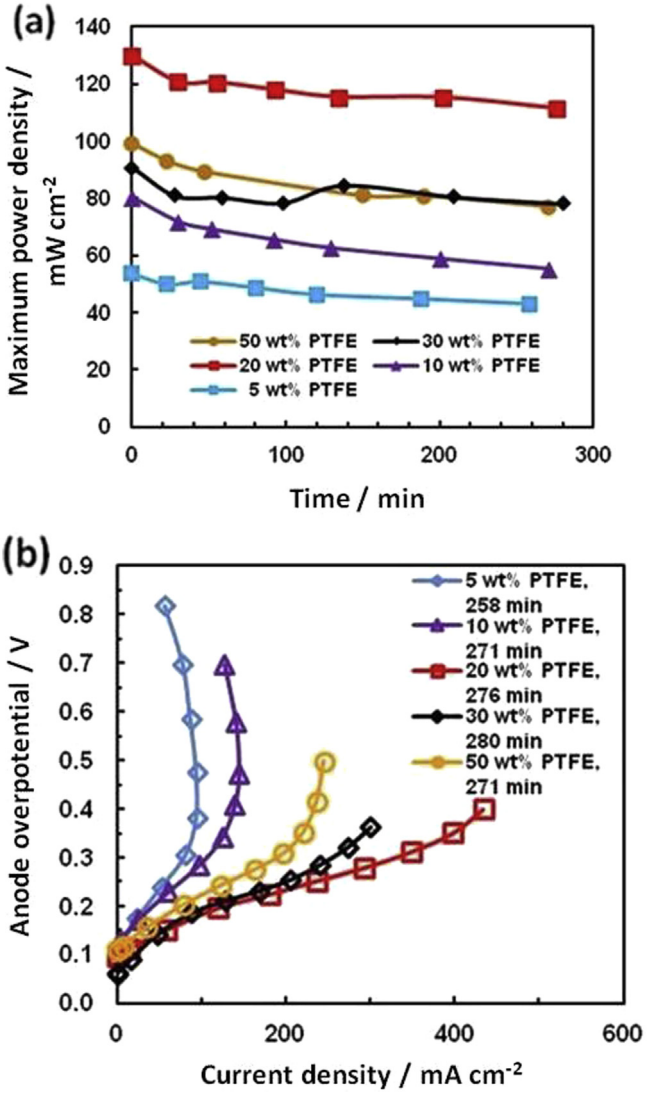

Fig. 4. (a) Maximum power density as a function of time and (b) final anode overpotentials as a function of current density with 0.4 V applied between polarization curves. Electrolyte: 3 M KOH. Electrolyte flow rate: 0.45 ml min^{-1}. Electrolyte thickness: 1.5 mm H_2/O_2 feeds: 50 SCCM. At room temperature.

point, the increased electrical resistance from increased wt% PTFE may have caused the decreased performance. The high anode overpotential (low cell voltage) behavior of the 5 wt% PTFE electrode, where increasing overpotential actually results in decreasing current, has been discussed in our previous work [9]. Our prior work explains that this "backwards" behavior of an alkaline anode was shown to be reproducible and reversible, possibly due to hydroxyl blocking at the anode at higher anode potentials. This behavior would be expected to be a larger problem for a less hydrophobic electrode, where the catalyst layer has more exposure to the electrolyte.

To test the stability of the various backing layers, the anodic performance of the backing layers was investigated over time in the microfluidic fuel cell. Potentially, the backing layers with higher PTFE content could show greater stability over time by preventing flooding. The electrolyte was recirculated over time for approximately 270 min using a pump. The cell was held at 0.4 V between polarization curves, which were taken periodically to acquire

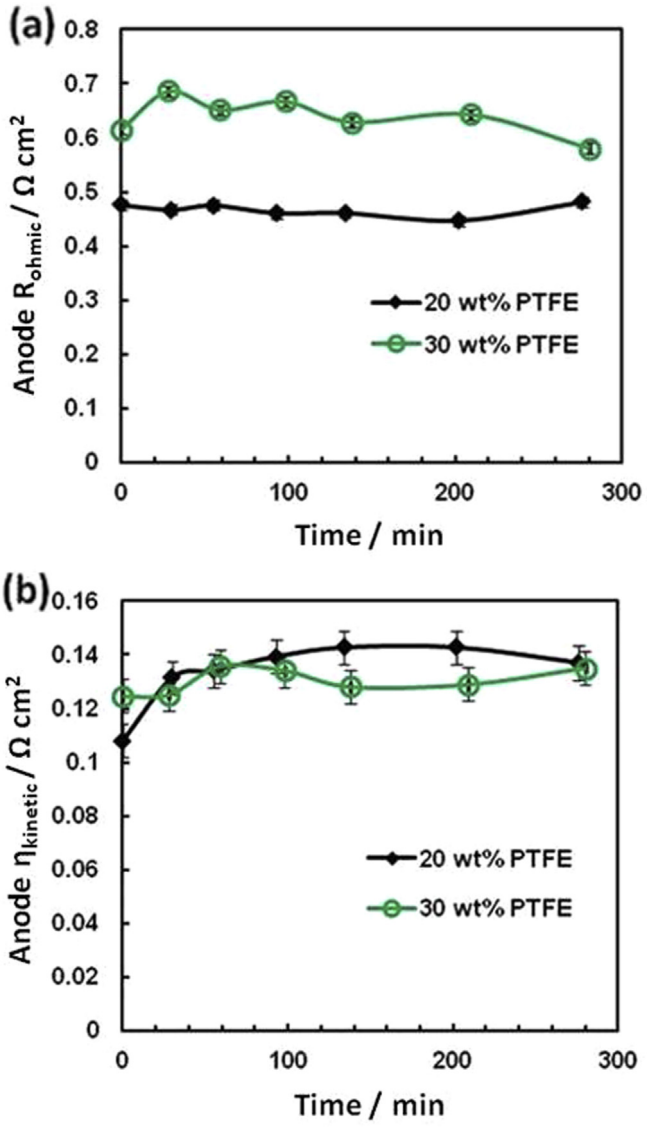

Fig. 5. (a) R_{ohmic} and (b) $\eta_{kinetic}$ as a function of time with 0.4 V applied between the polarization curves used to determine R_{ohmic} and $\eta_{kinetic}$. Error bars are standard error of 0.0093 Ω cm² for R_{ohmic} or 0.0062 V for $V_{kinetic}$, calculated from a triplicate repeat trial. Electrolyte: 3 M KOH. Electrolyte flow rate: 0.45 ml min^{-1}. Electrolyte thickness: 1.5 mm H_2/O_2 feeds: 50 SCCM. At room temperature.

Time / catalyst ink	0 min	60 min
No silicone oil	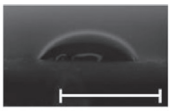	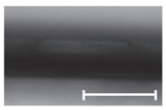
Silicone oil	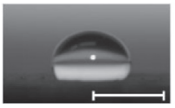	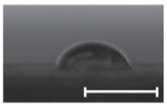

Fig. 6. Hydrophobicity of catalyst layers with and without silicone oil. Scale bar = 0.5 cm.

electrode potentials and power densities. The decline in power density over time is shown in Fig. 4a, with each curve showing similar trends. This result shows that increased wt% PTFE in a backing layer does not substantially improve power density stability over hours. This result may occur if flooding within the catalyst layer itself is limiting performance, in which case the

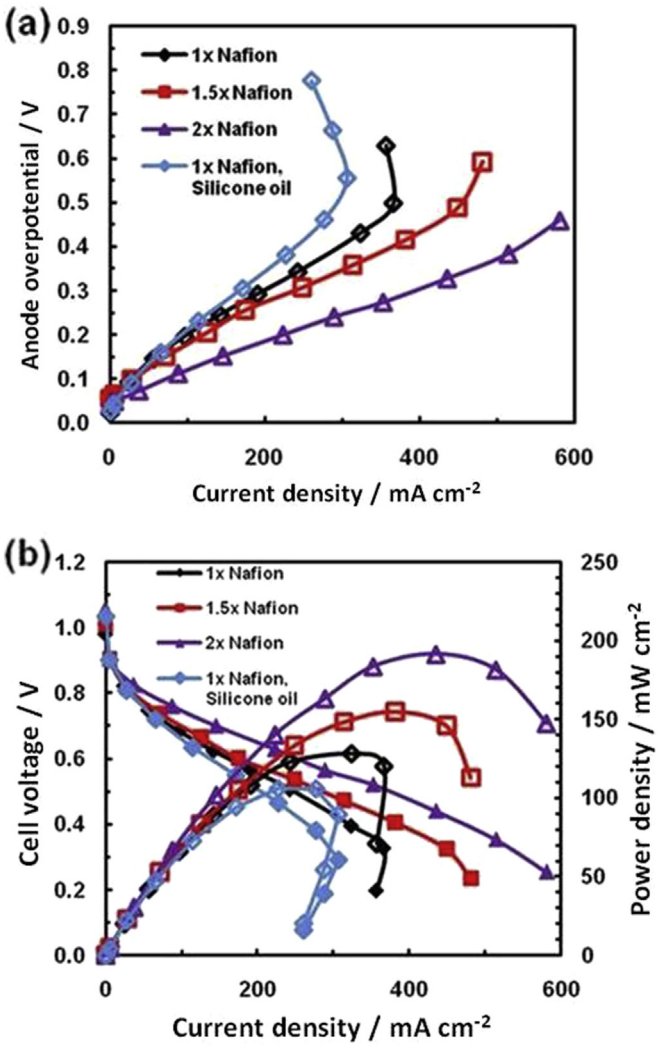

Fig. 7. (a) Anode overpotential and (b) polarization and power density curves as a function of current density. Electrolyte: 3 M KOH. Electrolyte flow rate: 0.45 ml min^{-1}. Electrolyte thickness: 1.5 mm H_2/O_2 feeds: 50 SCCM. At room temperature.

hydrophobicity of the backing layer does not play a role. The final anode overpotential curves (Fig. 4b) demonstrate that similar trends hold for the initial results and the results after extended operation. The combined results show that 20 wt% PTFE is optimal, which agrees with literature results for an acidic cathode, which also generates water, in a direct methanol fuel cell [12]. In addition, the 5 wt% PTFE backing layer electrode showed significantly larger amounts of water buildup than the other electrodes (Fig. S2).

Further investigation of R_{ohmic} and $\eta_{kinetic}$ was used to analyze the anode behavior. Using the previous data and applying individual electrode fits, the R_{ohmic} and $\eta_{kinetic}$ terms were studied over time with the 20 wt% PTFE and 30 wt% PTFE electrodes. In our previous work, these parameters were used to decouple the effects of mass transport and ohmic resistance from kinetic effects [9]. Fig. 5a shows that the superior performance of the 20 wt% PTFE anode is caused by a R_{ohmic} which is 27% lower than the 30 wt% PTFE anode. R_{ohmic} here is not purely based on the electrical resistance of the cell, but rather is the slope of the individual electrode plot in the ohmic region. From our previous work, a lower R_{ohmic} is caused by improved mass transport or ohmic behavior; in this case, improved mass transport is the likely explanation [9]. In this case, the lower R_{ohmic} is indicative of a less negative slope in the ohmic region of a full cell curve, caused by improved mass transport. As a result, 20 wt% PTFE was used for the remainder of these studies.

3.3. Altering catalyst ink hydrophobicity

The catalyst ink is another design area where the hydrophobicity can be altered. Work by Li et al. on acidic fuel cell cathodes suggests that increased hydrophobicity in the catalyst layer reduces overpotential [11]. The work suggested that silicone oil added to the catalyst layer would reduce overpotential by reducing flooding. An anode with 0.5 mg cm^{-2} silicone oil was synthesized to see if the performance increase from increased hydrophobicity would apply to an alkaline anode. Water droplet testing demonstrated that the silicone oil did significantly increase the hydrophobicity of the catalyst layer (Fig. 6). In addition, electrodes with increased Nafion wt% (3, 4.5, and 6) were synthesized as an alternate way to increase catalyst layer hydrophobicity. Although Nafion is often considered a hydrophilic polymer, it still is hydrophobic relative to the liquid electrolyte. Water droplet testing (not shown) did not show a major difference in catalyst layer hydrophobicity between electrodes that had 3 wt% Nafion and 6 wt% Nafion.

Fig. 7a shows that the overpotential increases notably when adding silicone oil to the anode catalyst layer. While the electrode with silicone oil performs similarly to the electrode without silicone oil at lower current densities, the overpotential difference becomes very apparent at current densities >200 mA cm^{-2}. This trend shows an increased R_{ohmic}, which indicates inferior mass transport when silicone is added. The likely explanation is that the silicone oil is partially preventing wetting of the catalyst layer, leading to mass transport losses. Although the addition of silicone oil did not reduce overpotential, increasing Nafion to 4.5 wt% (1.5× the original amount) or 6 wt% (2× the original amount) reduced anode overpotential significantly (Fig. 7a). Since Nafion does not conduct anions, this performance enhancement is attributed to increased anode hydrophobicity. A reduced R_{ohmic} leading to reduced overpotential is consistent with a mass transport explanation. Together, these results demonstrate that a liquid electrolyte fuel cell requires some hydrophobicity to keep the catalyst layer from entirely flooding, but still requires hydrophilicity to ensure proper electrolyte wetting.

3.4. Effect of gas flow rates on fuel utilization

The hydrogen supply rate can have a profound effect on anode performance. The supply of hydrogen plays a role in determining the maximum current density, as determined by Equation (1):

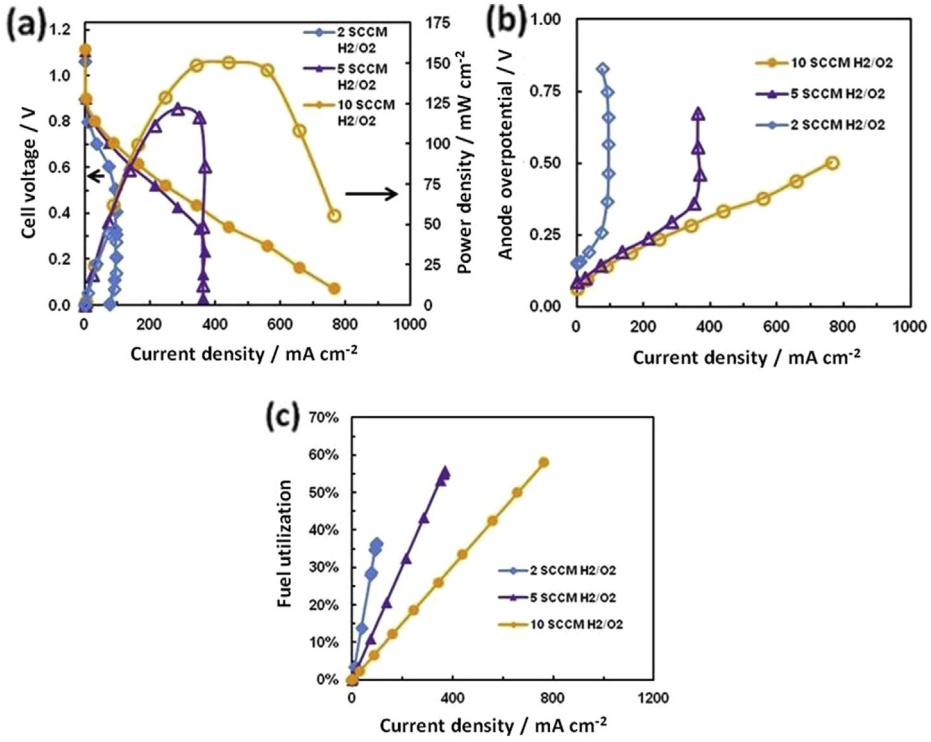

Fig. 8. (a) Polarization and power density curves, (b) anode overpotential, and (c) fuel utilization as a function of current density for varying H_2/O_2 flow rates. Electrolyte: 3 M KOH. Electrolyte flow rate: 0.45 ml min^{-1}. Electrolyte thickness: 1.5 mm. At room temperature.

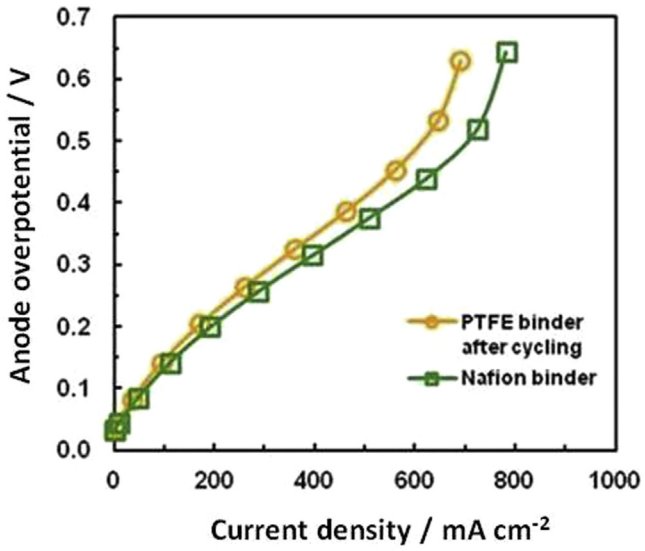

Fig. 9. Anode overpotential as a function of current density for PTFE and Nafion binders. Electrolyte: 3 M KOH. Electrolyte flow rate: 0.45 ml min^{-1}. Electrolyte thickness: 1.5 mm H_2/O_2 feeds: 10 SCCM. At room temperature.

$$\text{maximum current} = nF\left(\text{mol}\frac{H_2}{s}\right) \quad (1)$$

where: $n = 2$, the number of electrons per mol H_2

$F = 96{,}845$ C mol^{-1}, Faraday's constant

For 10 SCCM H_2, the maximum current is 1.32 Amps, while for 2 SCCM H_2, the maximum current is 263 mA. As the supply of hydrogen increases, the electrodes become the limiting factor, even at 0 V cell voltage. To investigate the effect of hydrogen supply, the top-performing anode (with 9 wt% PTFE) was tested in a fuel cell with H_2/O_2 flow rates varied from 2 to 50 SCCM. Fig. 8a shows a 20% drop in power density when dropping from 10 SCCM to 5 SCCM, and a 70% drop in power density when dropping from 10 SCCM to 2 SCCM. The corresponding anode overpotential curve (Fig. 9b) shows that the performance at 5 SCCM mirrors the performance at 10 SCCM at current densities $\leq$ 300 mA cm^{-2}, while 2 SCCM has significantly higher overpotential at all points. When considering fuel utilization (equivalent to the current density divided by the maximum current density based on H_2 flow rate), Fig. 9c shows that both 5 SCCM and 10 SCCM can reach almost 60% fuel utilization, while 2 SCCM is capped below 40%. The lower performance of the 2 SCCM implies that the concentration of H_2 plays a role in determining the overpotential and current density, as 5 SCCM and 10 SCCM would have higher concentrations near the electrode. This trend diverges sharply from results in acidic media (not shown), which show higher utilization at lower gas flow rates. However, the anode reaction in acidic media is much faster, so gas diffusion is more likely to be the limiting factor by itself.

3.5. Use of a PTFE binder

PTFE has been commonly used to bind electrodes in alkaline media [1]. In previous work, we have also used PTFE as a binder, in which the electrodes were painted with PTFE in the catalyst ink and then sintered in a tube furnace at 330 °C for 20 min. These electrodes were then voltage cycled to remove excess PTFE and thus enable wetting of the surface, as described in previous work [2]. Since the standard Nafion binder is designed for acidic media, two electrodes with Nafion and PTFE binders were compared in a short term polarization curve. Fig. 9 shows that although the PTFE-bonded electrode was able to achieve performance close to that of the Nafion bonded-electrode, the Nafion-bonded electrode was still superior. The minor difference in overpotential may be ascribed to the increased hydrophobicity of the PTFE-bonded electrode, which can be less desirable for the same reason as the silicone oil-

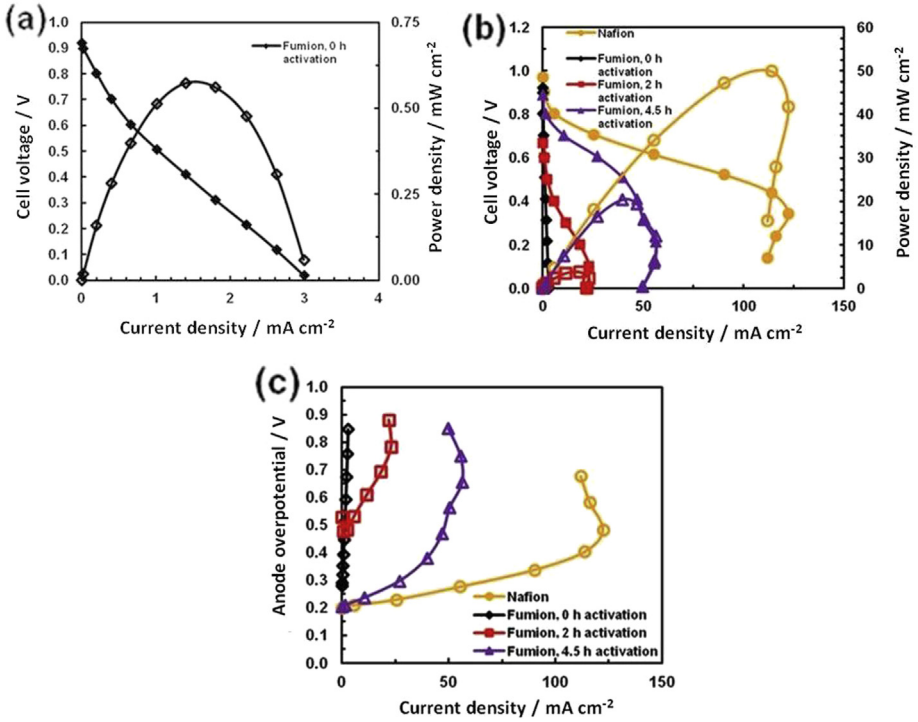

Fig. 10. (a) Initial polarization and power density curves, (b) final polarization and power density curves, and (c) anode overpotential as a function of current density for Fumion and Nafion electrodes with varying activation time. Electrolyte: 3 M KOH. Electrolyte flow rate: 0.6 ml min^{-1}. Electrolyte thickness: 2 mm. H_2/O_2 feeds: 50 SCCM. At room temperature.

treated electrode. It is also possible that a different catalyst layer structure, due to morphological differences between PTFE (microparticles) and Nafion (solution in alcohol-water mixture), is created by using the two different binders. Qualitative analysis of the catalyst layer by MicroCT imaging of electrodes using PTFE [16] and Nafion [17] as a binder shows similar catalyst layer structures. While PTFE is a viable binder in either case, the added cycling steps slow down electrode production. Thus, Nafion will usually be a superior choice even in alkaline media.

3.6. Use of an anion exchange binder

Using an ion-conductive binder can greatly reduce fuel cell overpotential. In acidic media, Nafion is routinely used as it conducts the protons from each electrode reaction. In alkaline media, Nafion does not have the same benefit, and serves largely as a binder that uptakes water/electrolyte. For this investigation, the anion-conductive polymer Fumion AMLD-alkaline was used as an alternate binder for Pt/C. Fumion, which is initially doped with Br^- anions, is dissolved in the solvent N,N-dimethylacetamide, so the ink was dissolved in N,N-dimethylacetamide instead of the standard 50:50 IPA:water mixture. Ion exchange of the binder to the OH^- form before painting was not attempted due to concerns about instability of the binder in the solvent. When using Toray electrodes, the N,N-dimethylacetamide soaked through the backing layer, causing flooding and electrolyte leaking (weeping). However, the Sigracet backing proved to be much more robust in the presence of N,N-dimethylacetamide, so it was used for the anode in these studies.

Initial testing of the Fumion anode yielded very poor results, with current densities $\leq$3 mA cm^{-2} and power density below 1 mW cm^{-2} (Fig. 10a). This result was attributed to the initial doping of the Fumion binder, which is initially doped with Br^- anions. Ion exchange of an electrode to the OH^- form by soaking in 7 M KOH resulted in damage to the electrodes from KOH weeping into the electrode backing layer. An alternative procedure was developed to substitute the electrode with OH^- anions, which are consumed in the anode reaction, by using the Fumion electrode as a cathode between trials in an activation procedure where the alkaline fuel cell was held at 0 V. After 2 h activation, a 6× jump in current density was observed and after 4.5 h activation, the Fumion electrode reached its maximum current density of 60 mA cm^{-2} (Fig. 10b). The corresponding individual anode parameters R_{ohmic} and $\eta_{kinetic}$ both decreased sharply as the activation proceeded (Fig. 10c). After 4.5 h activation, no further enhancement in performance was observed. While the activation procedure increased Fumion power density by a factor of 40, the analogous Nafion-bonded anode yielded 150% higher power density than the Fumion at its maximum. The anode R_{ohmic} was much lower for the Nafion-bonded electrode, indicating the anode losses for Fumion could again be due to the increased hydrophilicity of Fumion versus Nafion.

While this study shows Nafion outperforms the anion-exchange binder Fumion, other anion-exchange binders still have the potential to yield superior performance. The results here indicate that Nafion is superior because it is more hydrophilic; if an anion-exchange binder with similar hydrophilicity could be used, that binder would not be subject to the mass transport limitations found from using Fumion. At that point, the kinetic advantages from the extra OH^- anions could then greatly improve the kinetics. The key message here is that a proper amount of hydrophobicity is required for any binder to be viable in an alkaline fuel cell.

3.7. Use of PtRu/C

As part of the efforts to improve anode performance, a PtRu catalyst was tested at the anode. While PtRu is frequently used for carbon-based fuel oxidation, it is not routinely used for the

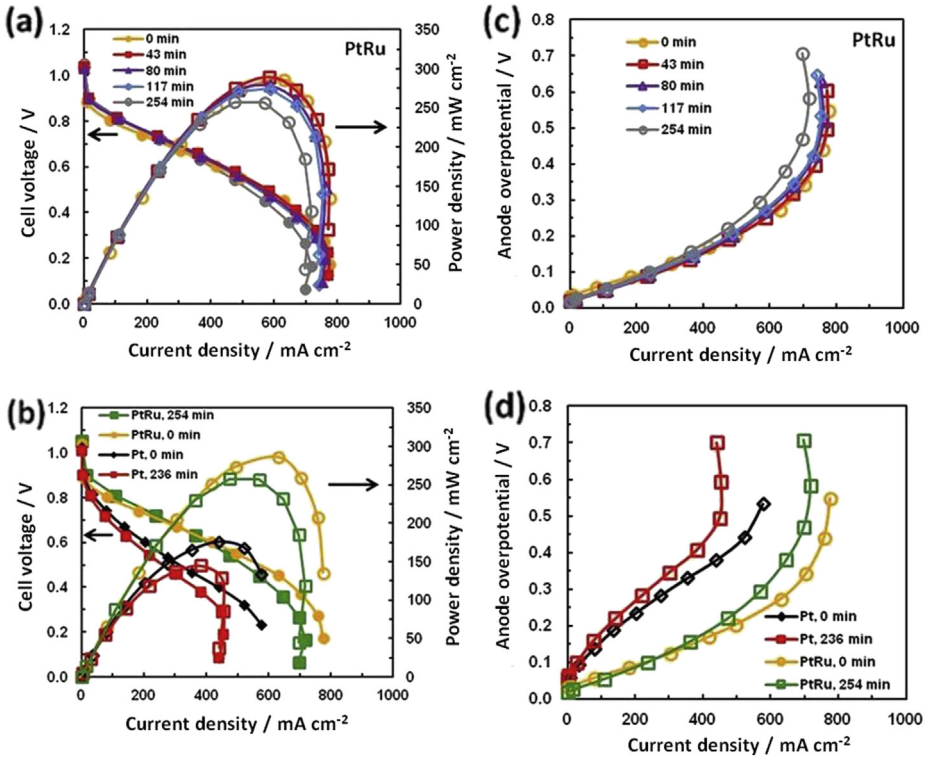

Fig. 11. Polarization and power density curves for (a) PtRu and (b) Pt vs PtRu as well as anode overpotential for (c) PtRu and (d) Pt vs PtRu as a function of current density over time with 0.4 V applied between polarization curves. Electrolyte: 3 M KOH. Electrolyte flow rate: 0.6 ml min^{-1}. Electrolyte thickness: 2 mm. H_2/O_2 feeds: 10 SCCM. At room temperature.

hydrogen oxidation reaction. Here, a PtRu anode was studied over time, where polarization curves were taken periodically and the cell was held at 0.4 V (the voltage for maximum power density) between experiments. Fig. 11a shows the high power density of 280 mW cm^{-2} achieved using the PtRu anode, which is the highest power density in alkaline media achieved from the microfluidic fuel cell to date. While the Pt cathode performance was stable over the course of the experiment, the PtRu anode overpotential did increase slightly, shown in Fig. 11c by an increase in R_{ohmic} likely caused by mass transport limitations from flooding. This trend persisted for the multiple PtRu anodes tested.

The PtRu electrode substantially outperformed a Pt electrode with an identical loading. Fig. 11b shows that the Pt electrode generates 203 mW cm^{-2}, 71% of the power density of the PtRu electrode. The PtRu electrode has a lower $\eta_{kinetic}$ by 80 mV and a lower R_{ohmic} by 33% (Fig. 11d); this type of change in both parameters is ambiguous, but could be kinetic or mass transport effects. Both electrodes demonstrated similar stability over approximately 4 h, with the result of an increase in R_{ohmic} due to mass transport losses.

There are several possible explanations for the improved PtRu performance. Potentially, PtRu could remove contaminants that could be limiting Pt/C electrode performance. It is also possible that the lower amount of carbon in the PtRu, as compared to the Pt, makes for a thinner catalyst layer with fewer gas transport issues.

4. Conclusions

In summary, we reported on experiments to determine the effects of altered electrode hydrophobicity, with the ultimate goal of improving electrode performance in alkaline media. Later batches of the Sigracet backing layer were found to induce flooding, while a similar Toray backing layer with 20 wt% PTFE was robust for both short term studies and extended trials. Increasing the hydrophobicity of the catalyst layer by increasing the Nafion wt% reduced overpotential, whereas use of the highly hydrophobic additive silicone oil increased overpotential. Use of Nafion binder led to superior performance compared to use of either non-conductive hydrophobic PTFE or anion-conductive hydrophobic Fumion. Finally, we also found that using an anode with PtRu/C as the catalyst yielded high power densities.

Understanding and being able to quantify the effects of hydrophobicity greatly benefits the investigation of alternate anode catalysts for operation in alkaline media. Specifically, the hydrophobicity of the backing and catalyst layer must be carefully controlled to prevent flooding, which is known to limit achievable current densities. Understanding the causes behind anode overpotential losses is necessary to improve the applicability of alkaline fuel cells as power sources. Looking forward, investigation of (i) PtRu/C catalysis at the anode and (ii) hydrophilic anion-conductive binders holds promise for further improvement of anodes for use in alkaline fuel cells.

Acknowledgments

We gratefully acknowledge financial support from the Department of Energy (DE-FG02005ER46260) and from the Dow Chemical Company for a graduate fellowship to MSN.

Appendix A. Supplementary material

Supplementary data related to this article can be found at http://dx.doi.org/10.1016/j.jpowsour.2013.05.054.

References

[1] G.F. McLean, T. Niet, S. Prince-Richard, N. Djilali, International Journal of Hydrogen Energy 27 (2002) 507–526.
[2] F.R. Brushett, W.P. Zhou, R.S. Jayashree, P.J.A. Kenis, Journal of the Electrochemical Society 156 (2009) B565–B571.
[3] E. Gülzow, Fuel Cells 4 (2004) 251–255.
[4] S. Gu, R. Cai, T. Luo, Z. Chen, M. Sun, Y. Liu, G. He, Y. Yan, Angewandte Chemie 121 (2009) 6621–6624.
[5] E. Gülzow, M. Schulze, Journal of Power Sources 127 (2004) 243–251.
[6] M. Cifrain, K.V. Kordesch, Journal of Power Sources 127 (2004) 234–242.
[7] L. Adams, S. Poynton, C. Tamain, R. Slade, J. Varcoe, ChemSusChem 1 (2008) 79–81.
[8] M.S. Naughton, F.R. Brushett, P.J.A. Kenis, Journal of Power Sources 196 (2011) 1762–1768.
[9] M.S. Naughton, A.A. Moradia, P.J.A. Kenis, Journal of the Electrochemical Society 159 (2012) B761–B769.
[10] L. Carrette, K.A. Friedrich, U. Stimming, Chemphyschem 1 (2000) 162–193.
[11] A. Li, M. Han, S.H. Chan, N.-t. Nguyen, Electrochimica Acta 55 (2010) 2706–2711.
[12] J. Zhang, L. Feng, W. Cai, C. Liu, W. Xing, Journal of Power Sources 196 (2011) 9510–9515.
[13] J.D. Fairweather, P. Cheung, D.T. Schwartz, Journal of Power Sources 195 (2010) 787–793.
[14] E.R. Choban, P. Waszczuk, P.J.A. Kenis, Electrochemical and Solid-State Letters 8 (2005) A348–A352.
[15] R.S. Jayashree, M. Mitchell, D. Natarajan, L.J. Markoski, P.J.A. Kenis, Langmuir 23 (2007) 6871–6874.
[16] F.R. Brushett, M.S. Naughton, J.W.D. Ng, L. Yin, P.J.A. Kenis, International Journal of Hydrogen Energy 37 (2011) 2559–2570.
[17] H.-R. Jhong, F.R. Brushett, L. Yin, D.M. Stevenson, P.J.A. Kenis, Journal of the Electrochemical Society 159 (2012) B292–B298.